

Band-offset trends in nitride heterojunctions

Nadia Binggeli and Philippe Ferrara*

Institut de Physique Appliquée, École Polytechnique Fédérale de Lausanne, PH-B Ecublens CH-1015 Lausanne, Switzerland

Alfonso Baldereschi

*Institut de Physique Appliquée and Institut Romand de Recherche Numérique en Physique des Matériaux (IRRMA),
and École Polytechnique Fédérale de Lausanne, PH-B Ecublens, CH-1015 Lausanne, Switzerland
and Dipartimento di Fisica Teorica and INFN, Università di Trieste, I-34014 Trieste, Italy*

(Received 21 December 2000; published 30 May 2001)

From first principles we have examined the band offsets of selected zinc-blende, wurtzite, and mixed zinc-blende/wurtzite GaN/AlN, GaN/SiC, and AlN/SiC heterostructures, and their dependence on various structural and chemical properties of the interfaces. Contrary to the case of the conventional, small-gap, semiconductor heterojunctions, local atomic interfacial relaxation has a major influence on the offsets of the polar heterovalent nitride systems. However, provided this effect is taken into account, the band-offset dependence on interface orientation, strain, and heterovalency can still be qualitatively explained using linear-response-theory schemes. We also show that a change in the band-gap discontinuity resulting from a cubic (111) to hexagonal (0001) polytype transformation in nitride heterostructures will be selectively found in the conduction-band offset.

DOI: 10.1103/PhysRevB.63.245306

PACS number(s): 73.20.-r, 73.40.Kp, 73.40.Lq

I. INTRODUCTION

The wide-gap nitrides, and in particular GaN, are materials of high interest for device applications in blue-violet optoelectronics and high-temperature electronics.¹ All GaN-based devices demonstrated to date were fabricated by heteroepitaxy on sapphire or SiC substrates, in view of the low availability of the group-III nitride single crystals. With respect to sapphire, SiC exhibits a much smaller lattice mismatch with GaN (3.5 % versus ~ 14 %) and more similar thermal expansion characteristics, which are expected to give rise to superior device performances. The existence of an almost perfect lattice matching between SiC and AlN also makes AlN a suitable buffer layer for GaN epitaxy on SiC.² The main parameters which govern the transport properties and quantum confinement in the resulting heterostructures are the valence- and conduction-band discontinuities at the interfaces. Presently, little experimental data and large uncertainties exist on the band offsets at nitride interfaces.^{3–11} Theoretical values have been reported for some isovalent heterojunctions,^{12–17} but are still scarce for heterovalent systems,^{18–21} and little is known yet about the structural and chemical trends of these offsets as compared to those in other semiconductor heterojunctions.

For conventional, smaller-gap, semiconductor systems, predictions based on linear-response theory, such as the transitivity of the band-discontinuities at isovalent lattice-matched interfaces, provide an accurate description of the band-offset trends.²² For nitrides and related wide-gap materials, however, it is unclear to what extent linear-response-theory models still apply, because of the large ionicity of the materials involved. Furthermore, even for GaN/AlN, which is the most studied among the nitride heterojunctions, conflicting theoretical results exist concerning the effects of strain and local interfacial atomic relaxation on the band offsets in pseudomorphic heterostructures.^{14,16}

Another important issue concerning the wide-gap heterojunctions is the effect of polytypes. Materials such as GaN, AlN, and SiC can be grown either in hexagonal or cubic crystalline forms, with substantially different band gaps. It was suggested¹⁵ that, due to the relative similarity of the valence-band-edge states in cubic and hexagonal structures, the average valence-band offset (VBO) may not be very sensitive to polytype. Although this is in general agreement with the result of previous *ab initio* calculations for zinc-blende and wurtzite GaN/AlN heterojunctions,^{12,17} the systematics of this behavior has not yet been established.

In this paper, by means of first-principles calculations we study the band-offset properties in nitride-based heterostructures. As prototype systems, we consider isovalent GaN/AlN and heterovalent GaN/SiC and AlN/SiC heterojunctions with crystalline forms of increasing complexity, going from zinc-blende to wurtzite, and to mixed zinc-blende/wurtzite heterostructures. We examine the band-offset dependence on interface orientation, strain, heterovalency, and polytype. Our results indicate that, contrary to the case of the conventional semiconductor heterojunctions, local atomic interfacial relaxation has a major influence on the offsets of the polar heterovalent nitride interfaces. We also show, however, that provided this relaxation is taken into account, the band-offset dependence on interface orientation, strain, and heterovalency can still be qualitatively explained using linear-response-theory schemes. Polytype effects will be discussed in connection with the effect of stacking faults in zinc-blende/wurtzite heterojunctions, and will be shown to selectively affect the conduction-band offsets.

II. COMPUTATIONAL METHOD

The calculations were performed within the local-density approximation (LDA) to density-functional theory, using the pseudopotential plane-wave method. We employed the

exchange-correlation functional of Ceperley and Alder, as parametrized by Perdew and Zunger.²³ The pseudopotentials were generated with the method of Troullier and Martins.²⁴ For Ga, we generated two types of pseudopotentials with the Ga-3*d* orbitals treated either as core states or as valence states. For the construction of the pseudopotentials, as a reference configuration we used the valence-ground state of the non-spin-polarized atoms, and we employed the following core radii cutoffs (in a.u.): $r_s=r_p=1.5$ for C, $r_s=r_p=1.45$ for N, $r_s=r_p=r_d=1.8$ for Al and Si, and $r_s=r_p=1.65(2.0)$, $r_d=1.65(2.4)$, and $r_f=2.0(2.4)$ for Ga, with the Ga-3*d* orbitals treated as valence (core) states. The pseudopotentials were then cast into the Kleinman-Bylander²⁵ nonlocal form using the *p* orbital as local component for all elements except Ga, for which the *f* orbital was used. Unless otherwise stated, the results in the following sections correspond to calculations treating the Ga-3*d* orbitals as valence states.

The heterojunctions were modeled with supercells containing up to 24 atoms, i.e., up to 6 ML of each material for the cubic (110) heterojunctions, and 12 ML of each material for the cubic (100), (111) and hexagonal (0001) heterojunctions. The supercell calculations were carried out with a plane-wave kinetic-energy cutoff of 60 Ry for systems with no Ga atom or when the Ga-3*d* orbitals were treated as core states. A cutoff of 100 Ry was used, instead, when the Ga-3*d* orbitals were treated as valence states. The *k*-space integrations were performed with (4,4,1), (4,2,1) and (3,3,1) Monkhorst-Pack grids²⁶ for the (100), (110) and (111) junctions, respectively. For the hexagonal (0001) junctions, we used the same grid as for the cubic (111) junctions.

Most of our calculations were performed for heterostructures pseudomorphically grown on a SiC substrate. For the in-plane lattice parameter, we used the calculated value of the SiC equilibrium lattice constant, namely, $a_{\text{SiC}}(3\text{C})=4.32$ Å for the zinc-blende heterostructures and $a_{\text{SiC}}(2\text{H})=3.06$ Å for the wurtzite heterostructures; the experimental values for the cubic and hexagonal phases are 4.36 and 3.08 Å, respectively.²⁷ We neglected the small difference (less than 1%) between the equilibrium lattice constants of AlN and SiC, and treated these materials as lattice matched. For the lattice parameter along the growth direction in the AlN/SiC(0001) wurtzite heterojunction, we used the SiC theoretical equilibrium lattice constant: $c_{\text{SiC}}(2\text{H})=4.99$ Å; the experimental values are 5.05 Å and 4.98 Å for SiC and AlN, respectively.^{27,28}

For GaN, the calculated equilibrium lattice parameters obtained with the Ga-3*d* electrons treated as valence electrons are $a_{\text{GaN}}(3\text{C})=4.46$ Å, $a_{\text{GaN}}(2\text{H})=3.15$ Å, and $c_{\text{GaN}}(2\text{H})=5.14$ Å. These values compare well with the experimental values $a_{\text{GaN}}^{\text{expt}}(3\text{C})=4.50$ Å, $a_{\text{GaN}}^{\text{expt}}(2\text{H})=3.19$ Å, and $c_{\text{GaN}}^{\text{expt}}(2\text{H})=5.18$ Å.²⁸ They yield an in-plane misfit $\epsilon_{\parallel}=\Delta a/a$, between GaN and AlN (or SiC) of $\sim 3\%$, consistent with experiment. The tetragonal deformation of the overlayers in pseudomorphic heterojunctions were obtained from macroscopic elasticity theory, using the theoretical values of the elastic constants given in Ref. 29.

The equilibrium lattice parameters of GaN determined

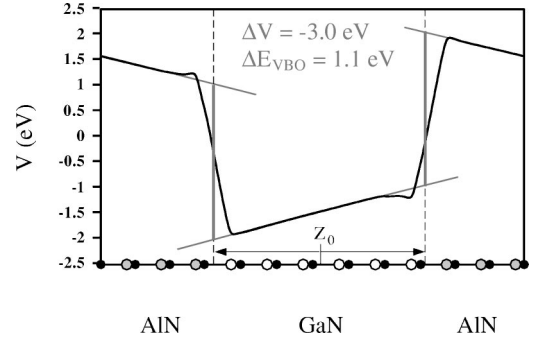


FIG. 1. Macroscopic average of the electrostatic potential in the GaN/AlN(0001) junction coherently strained to the AlN lattice parameter. Z_0 indicates the midpoint between the charged interface planes; the theoretical positions of the interface planes are indicated by dashed lines, and are used to measure the potential discontinuities (see text). The resulting values of ΔV and E_{VBO} are also shown.

from calculations treating the Ga-3*d* orbitals as core states are $a_{\text{GaN}}(3\text{C})=4.35$ Å, $a_{\text{GaN}}(2\text{H})=3.08$ Å, and $c_{\text{GaN}}(2\text{H})=5.01$ Å. These values differ by less than 1% from the theoretical values obtained for SiC and AlN. Therefore, in all calculations treating the Ga-3*d* electrons as core electrons, we neglected the small misfits between the theoretical equilibrium lattice parameters of GaN, AlN, and SiC, and used the calculated values of the SiC lattice constants.

The VBO was evaluated as $\Delta E_{VBO}=\Delta E_v+\Delta V$,^{22,30} where ΔE_v is the difference between the valence-band maxima of the two semiconductors, each measured with respect to the average electrostatic potential in the corresponding crystal, and ΔV is the lineup of the average electrostatic potentials at the interface. ΔE_v is independent of interface-specific features, and was obtained from standard bulk band-structure calculations using an energy cutoffs of 70 Ry (120 Ry with the Ga-3*d* electrons) and a (4,4,4) Monkhorst-Pack mesh. Spin-orbit splittings were not considered, as they are very small (less than 20 meV) in SiC and in the nitrides.^{12,31} ΔV may depend on interface-specific features, and was derived via Poisson's equation from the self-consistent charge density in the supercell, using the macroscopic-average technique.²²

For ferroelectric and/or strained piezoelectric systems, such as the AlN/GaN (0001) wurtzite and (111) zinc-blende heterojunctions, macroscopic polarization charges are present at the interfaces. These charges, which are opposite at the two inequivalent interfaces of the supercells, produce a sawtooth electrostatic potential profile which complicates the evaluation of the potential step ΔV (Fig. 1). In the specific case of a mathematical dipole (point dipole at the interface), the corresponding discontinuity can be trivially measured in the presence of macroscopic charges or electric fields by fitting with two straight lines the macroscopic averaged potential $\bar{V}(z)$ in the two bulk materials, and determining their intersections with the interface plane. In a real system, however, the interface region is often broad and the dipole position is not clearly defined at a charged interface. Some reasonable criteria have to be introduced thus to position at best the interface planes.

TABLE I. Valence-band offsets (in eV) in pseudomorphic GaN/AlN zinc-blende heterojunctions on an AlN substrate. The numbers in parentheses show results from calculations treating the Ga-3*d* orbitals as core states. Ideal configurations refer to heterojunctions generated using the AlN lattice parameter, and neglecting local atomic relaxation at the interface.

GaN/AlN	(110)	(100)	(111)
Pseudomorphic	0.94 (0.79)	0.98 (0.75)	1.07 (0.80)
Ideal	1.08 (0.87)	1.07 (0.88)	1.06 (0.87)

In the problematic cases of the GaN/AlN (0001) and (111) junctions, we started by assuming identical discontinuities at the two charged interfaces of the supercell. This condition, which is physically reasonable, fixes the distance between the two interface planes in the supercell. We then determined the position of the midpoint, z_0 , between the two interface planes using a criterion of optimally localized monopoles proposed in Ref. 16. With this criterion one minimizes the spreading of a monopole density obtained from the difference between the macroscopic charge density of one of the interfaces and that of the other interface after reflection about z_0 .¹⁶ Using this scheme to position the interface planes, the potential discontinuities were then derived using the procedure that we described above for the point dipoles (see Fig. 1).

Our overall uncertainty on the absolute values of the calculated VBO's is estimated as ~ 0.2 eV, and derives mainly from neglecting many-body effects within the LDA.³² As usual, however, within the LDA, a better accuracy of the order of our numerical uncertainty (~ 50 meV) is expected on the variations of the VBO's with different interface-specific properties.³⁰

III. ZINC-BLENDE HETEROJUNCTIONS

A. Isovalent interfaces

1. GaN/AlN band offset: orientation dependence

In Table I, we display our values for the GaN/AlN (100), (110), and (111) VBO's, determined for GaN coherently strained to AlN. The results are given with (pseudomorphic) and without (ideal) a tetragonal deformation of the overlayer and local atomic relaxation at the interface. The differences between the values for the strained and ideal interfaces are of the order of 0.1 eV. Using the experimental bandgap value of 3.2 eV for 3C-GaN and a bandgap estimate of 4.9 eV for 3C-AlN,³³ we find a band alignment of type I in all cases.

The VBO differences between the strained (100), (110), and (111) interfaces range from 0.04 to 0.13 eV. These differences are a combined effect of bulk strain in the overlayer and local atomic relaxation at the interface. Neglecting these two effects, the VBO is essentially independent of interface orientation (see Table I).³⁴ Many-body corrections on the GaN and AlN bulk-band structures could change the absolute value of the VBO by 0.1–0.2 eV.³² Such corrections,

however, are not expected to affect the type of band alignment or the VBO dependence on interface-specific features, such as interface orientation.

Our VBO values in Table I are consistent with previous calculations for the GaN/AlN (100),^{12,14,17} (110),^{13,17,15} and (111) heterojunctions,¹⁷ taking into account the effect of different strain conditions^{12,13,15} and/or different treatments of the Ga-3*d* electrons.^{13,14,17} We will compare our results to previous data in more detail in Sec. III A 2, after having examined the effects of strain and of different treatments of the Ga-3*d* electrons.

The very small variation of the VBO we find with interface orientation seems to indicate that the band alignment at these isovalent nitride interfaces is controlled essentially by the bulk properties of the constituents, as opposed to interface-specific properties. In order to check this point, we have first examined the nature of the Ga-3*d* contribution to the VBO, obtained from separate calculations performed with the Ga-3*d* orbitals treated as core states. We then probed the nature of the potential lineup, free from Ga-3*d* effects, using an approach based on linear-response theory.

The results of the computations treating the Ga-3*d* orbitals as core states are shown in Table I. The Ga-3*d* semicore states increase the VBO, as expected from the upward shift of the N(2*p*)-like valence-band-edge states in bulk GaN, produced by the N(2*p*)-Ga(3*d*) level repulsion.³⁵ Neglecting local atomic relaxation, the calculated 3*d* shift of the VBO is essentially the same for the three different interface orientations, and amounts to 20 ± 1 meV. Furthermore, this shift is virtually identical to the value of 0.21 meV that we find for the VBO of a fictitious GaN(3*d*-valence)/GaN(3*d*-core) (110) homojunction that includes Ga-3*d* orbitals treated as valence states on one side of the junction and as core states on the other side of the junction. This shows that, neglecting atomic relaxation, the Ga-3*d* shift is purely a bulk effect in these isovalent nitride systems.

We also evaluated the effect of the Ga-3*d* electrons on the VBO by including the so-called non-linear-core correction (NLCC) for the exchange-correlation potential in calculations treating the Ga-3*d* electrons as core orbitals.³⁶ With this approximation, the change in the VBO is only 0.10 eV. The NLCC thus accounts for only half of the total bulk shift produced by the Ga-3*d* electrons on the GaN/AlN VBO.

The nature of the potential lineup, without the Ga-3*d* contribution, was then examined using a linear-response-theory (LRT) scheme.^{22,37} In this approach, the GaN/AlN interface is considered as a perturbation with respect to a reference bulk system, taken here as bulk GaN. Within the LRT scheme, the charge density, and hence the potential lineup, of the interface is fully determined by the electronic response of bulk GaN to a single atomic substitution transforming a Ga ion into an Al ion. The validity of the LRT model is tested in Fig. 2 for the AlN-GaN system. In Fig. 2(a), we show the self-consistent charge density and electrostatic potential induced by a Ga \rightarrow Al (100) cation-plane substitution in bulk GaN, together with the LRT result corresponding to a linear superposition of the responses to single Ga \rightarrow Al atomic substitutions. We computed the response to a single Ga \rightarrow Al atomic substitution in a bulk GaN using a supercell

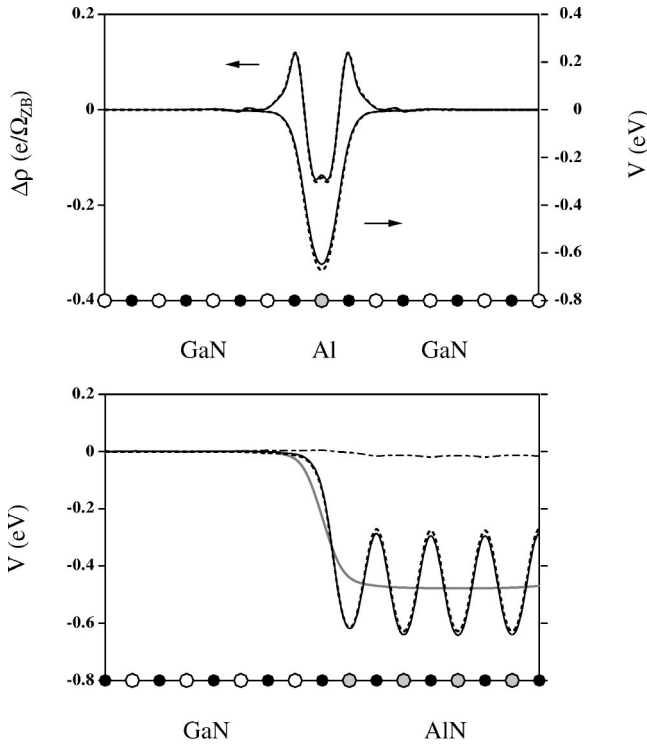


FIG. 2. Upper panel: planar averages of the valence charge density and electrostatic potential induced by an Al(100) single layer substitution in bulk GaN. The charge density and electrostatic potential obtained from a linear superposition of responses to single Al \rightarrow Ga atomic substitutions are also indicated (dashed lines). Lower panel: linear superposition of the electrostatic potentials induced by Al (100) single-layer substitutions in bulk GaN (planar average: solid dark line; macroscopic average: solid gray line) compared to the electrostatic potential induced by a full slab of AlN in GaN (planar average: dashed dark line; macroscopic average: dashed gray line). The difference between the two potential lineups is also indicated (dotted line).

including 32 atoms. The difference between the exact and the LRT result is barely visible in the figure.

Similarly, in Fig. 2(b), we compare the self-consistent electrostatic potential step induced by a slab of AlN in GaN to the electrostatic potential resulting from a linear superposition of the responses to single Ga \rightarrow Al cation-plane substitutions in bulk GaN. Also in this case, the difference is negligible. In fact, we find that the potential lineup determined from the superposition of bulk responses to the single atomic substitutions reproduces to within 0.02 eV the values calculated self-consistently for the three interfaces. This demonstrates the bulk nature of the GaN/AlN potential lineup, and hence of the GaN/AlN band offset. The band offset is therefore expected to be insensitive not only to interface orientation, but more generally to any interface-specific perturbation associated with a local neutral rearrangement of the atomic structure at the interface. This includes interfacial roughness as well as cation alloying near the interface.

It is interesting to note that although nonlinear contributions originating from *intersite* interactions are negligible for the common-anion GaN/AlN system, the electronic response to the single Ga \rightarrow Al atomic substitution is highly nonlinear.

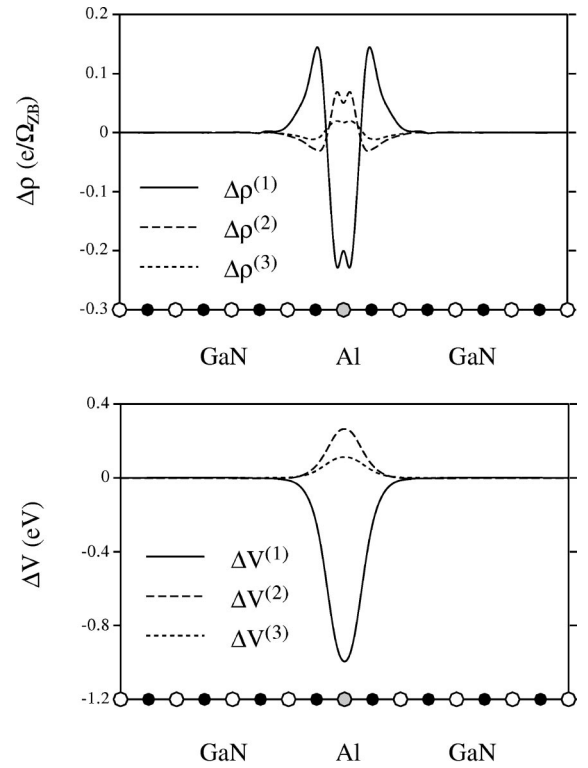


FIG. 3. Planar averages of the valence-charge-density (upper panel) and electrostatic-potential (lower panel) responses to an AlN(100) planar substitution in GaN. Linear, quadratic, and higher-order responses are indicated by solid, dashed, and dotted lines, respectively.

This is illustrated in Fig. 3, where we show the linear, quadratic and higher-order contributions (calculated within the virtual-crystal approximation³⁰) to the charge density and electrostatic potential induced by the single Ga \rightarrow Al (100) planar substitution in GaN. There is a substantial quadratic effect, and even the higher-order contributions are non-negligible. This behavior is at variance with that of the conventional semiconductor heterojunctions, such as GaAs/AlAs, where the electronic response to the Ga \rightarrow Al substitution is essentially linear in the perturbation.³⁷

Figure 3 also shows that the nonlinear contributions to the charge density induced by the cation substitutions extend significantly in the region of the nearest-neighbor N ions. This suggests that the presence of a common ion, and hence the absence of nearest-neighbor intersite interaction, is essential to insure a bulk behavior of the band alignment in these highly ionic systems. A common anion is present in all isovalent nitride heterojunctions, but not at heterovalent nitride interfaces. The results in Fig. 3 suggest the existence of non-negligible deviations from bulk trends (transitivity rule), induced by nearest-neighbor intersite interactions, at the non-polar heterovalent nitride interfaces. We will come back to this point in Sec. III B 1.

2. Strain dependence of the GaN/AlN band offset

The strain dependence of the VBO in pseudomorphic GaN/AlN(100) heterostructures is illustrated in Fig. 4. The

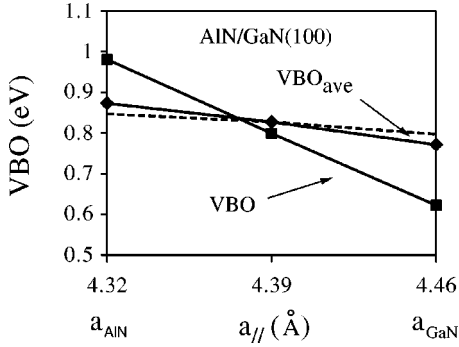


FIG. 4. Valence-band offset (VBO) in pseudomorphically strained AlN/GaN(100) heterojunctions as a function of the substrate lattice parameter. VBO_{ave} indicates the VBO measured between the average of the valence-band-edge manifolds in GaN and AlN. The solid line shows the results of the *ab initio* calculations, and the dashed line shows the strain dependence of VBO_{ave} predicted using the calculated deformation potentials of GaN and AlN (see the text).

strain resulting from a change in the substrate from AlN to GaN (3% misfit) reduces the band offset by as much as 0.35 eV. Most of the change in the VBO is due to the strain-induced splitting of the valence-band-edge manifolds in bulk GaN and AlN. The change with strain in the offset measured between the average of the split-valence-edge states (VBO_{ave}) of GaN and AlN is only 0.09 eV (see Fig. 4).

The strain-induced splittings of the valence-band-edge states in cubic semiconductors are determined, in the linear regime, by the deformation potentials b and d .³⁸ Taken separately, b and d determine the splittings produced by (100) and (111) uniaxial strains, respectively. From linear-response calculations for bulk GaN and AlN, we obtain

$$b^{AlN} = -1.4 \text{ eV}, \quad d^{AlN} = -5.6 \text{ eV} \quad (1)$$

and

$$b^{GaN} = -1.6 \text{ eV}, \quad d^{GaN} = -4.4 \text{ eV}. \quad (2)$$

These deformation potentials are in reasonable agreement with the values obtained by van de Walle and Neugebauer¹³ and Kim *et al.*²⁹ from *ab initio* computations. The largest difference concerns the value of d^{AlN} for which van de Walle and Neugebauer found -4.5 eV. Kim *et al.*, instead, obtained a value of -5.3 eV, more similar to our result.

The values of the uniaxial deformation, $\epsilon_{\perp} - \epsilon_{\parallel}$, of GaN on AlN in the coherently strained GaN/AlN (100), (110), and (111) heterostructures are 6%, 4%, and 4%, respectively. Using these values, together with our computed values for b^{GaN} and d^{GaN} , we obtain a band-edge-splitting contribution to the VBO of +0.10 eV for the (100) and (111) interfaces, and one of +0.12 eV for the (110) interface. These results reproduce to within 10 meV the splitting contributions to the VBO's of the coherently strained heterostructures studied in Sec. III A 1. Using our values for b^{AlN} and b^{GaN} , we also reproduce, to within 20 meV, the variation of VBO- VBO_{ave} (100) with the substrate, from AlN to GaN, displayed in Fig. 4.

Furthermore, we find that even the variation with strain of VBO_{ave} in Fig. 4 is determined mainly by the bulk properties of GaN and AlN, namely, by their volume changes and absolute band-edge deformation potentials. The absolute band-edge deformation potential for uniaxial strain is defined as $D_{v,ave}(\hat{n}) = dE_{v,ave}/d\epsilon$, where $E_{v,ave}$ is the average energy of the split-valence states, ϵ is the uniaxial strain, and \hat{n} is its direction.³⁹ For a given uniaxial strain, the deformation potential in a nonpolar system has been shown to be a bulk property,⁴⁰ which can be computed at a strained-unstrained homojunction.³⁹ For the nonpolar (110) orientation of GaN and AlN, in particular, using a supercell including 20 atoms (five strained planes plus five unstrained planes), we find⁴¹

$$D_{v,ave}^{AlN}(110) = 3.5 \text{ eV}, \quad D_{v,ave}^{GaN}(110) = 2.2 \text{ eV}. \quad (3)$$

For the polar (100) orientation, however, the GaN and AlN deformation potentials depend, in principle, on the details of the surface geometry because of the presence of nonvanishing Born effective charges.⁴⁰ A procedure to obtain a bulk (100) deformation potential, which is free from effective-charge effects, is to average the deformation potentials computed for two strained-unstrained (100) homojunctions with interchanged cations and anions.⁴² With this procedure, and using a supercell containing 20 atomic planes, we obtain

$$\bar{D}_{v,ave}^{AlN}(100) = 2.2 \text{ eV}, \quad \bar{D}_{v,ave}^{GaN}(100) = 0.7 \text{ eV}. \quad (4)$$

Using these values together with a 3% volume increase in GaN and AlN, due to the change in substrate from AlN to GaN, we predict a variation of -0.05 eV in VBO_{ave} , in reasonable agreement with the variation of -0.09 eV obtained from the self-consistent results in Fig. 4.

We note that for pseudomorphic structures, the variation of VBO_{ave} with the substrate is controlled essentially by the difference $D_{v,ave}^{AlN} - D_{v,ave}^{GaN}$. Our results, in Eqs. (3) and (4), indicate that this difference ($\sim 1.4 \pm 0.1$ eV) is not very sensitive to the crystallographic orientation. This difference may thus be used also to obtain estimates of the VBO change for other substrate orientations.

van de Walle and Neugebauer computed the deformation potentials $D_{v,ave}^{AlN}$ and $D_{v,ave}^{GaN}$ for the nonpolar (110) orientation, using a pseudopotential approach and a NLCC for Ga.¹³ Our values agree with theirs to within ~ 1 eV (which may not be considered as a bad agreement for a quantity such as the absolute deformation potential³⁸). For the relative value $D_{v,ave}^{AlN}(110) - D_{v,ave}^{GaN}(110)$, however, van de Walle and Neugebauer obtained 0.3 eV, which is much smaller than what we find (1.5 eV). This difference may be explained in part by the different treatment of the Ga-3*d* electrons in the two calculations. In fact, we find that when the Ga-3*d* orbitals are treated as core states the GaN (100) and (110) deformation potentials increase by 0.6 eV, which reduces the difference between the AlN and GaN deformation potentials by a factor of 2.

We note in this connection that the values reported for the deformation potentials in Eqs. (1)–(4) were computed at the reference average lattice parameter of AlN and GaN ($a = 4.39$ Å). However, changing the lattice parameter from its

average value to its value in bulk AlN (GaN) modifies the deformation potentials by no more than 0.2 eV. Such a change decreases $D_{ave}^{AlN(GaN)}$ by 0.1 eV, decreases (increases) $d^{AlN(GaN)}$ by 0.2 eV, and leaves $b^{GaN(AlN)}$ unchanged.

Our results for the pseudomorphic (100) heterojunctions, in Fig. 4, are consistent with the value of 0.84 eV determined by Wei and Zunger from LAPW calculations, using as in-plane lattice parameter the average between the GaN and AlN lattice constants.¹² For an AlN substrate, Majewski and Stadele found a value of 0.75 eV. Nardelli *et al.*¹⁴ obtained values of 0.73 and 0.44 eV for AlN and GaN substrates, respectively. Both studies were based on pseudopotential calculations treating the Ga-3*d* orbitals as core states and using a NLCC. The resulting values are somewhat shifted to lower energy with respect to our values, as expected from the influence of the Ga-3*d* electrons. However, the variation of the VBO with the substrate parameter is in good agreement with our result.

Albanesi *et al.* found a value of 0.85 eV for the VBO of the GaN/AlN(110) junction, from calculations performed using the GaN lattice parameter and neglecting local atomic relaxation at the interface.¹⁵ This value is about 0.2 eV smaller than our value in Table I for the ideal AlN/GaN(110) interface. This difference results from the change in the lattice constant. Performing the calculations, as Albanesi *et al.* did, at the GaN instead of the AlN lattice parameter, we find a value of 0.90 eV, similar to their value.⁴³

Based on our results for the bulk GaN and AlN deformation potentials and for the offsets of the coherently strained GaN/AlN heterojunctions, we are in a position to propose an estimate for the offset of the strain-relaxed heterojunctions. The assumption here is that, similarly to the case of the pseudomorphic systems, the band offset of the relaxed system is controlled by bulk properties. Starting from the VBO_{ave} value for the strained GaN/AlN(100) heterojunction with the average GaN-AlN in-plane lattice parameter (0.83 eV), and using our deformation potential in Eqs. (4) together with a 1.5% volume increase (decrease) for GaN (AlN), we obtain a value of 0.87 eV for the VBO of the relaxed GaN/AlN(100) system. We note that if the junction with the AlN or GaN substrate had been used as a reference system in the calculation, this would change our prediction by 20 meV at most.

To the best of our knowledge, no experimental measurements have yet been performed for the band offsets of the GaN/AlN zinc-blende heterojunctions. However, our value for the relaxed GaN/AlN zinc-blende system compares reasonably well with the range of experimental data on the offsets of the wurtzite AlN/GaN heterojunctions.^{3–8} We will discuss this point more extensively in Sec. V, after having examined the wurtzite heterostructures (Sec. IV).

Finally, we would like to caution the reader that, although for the isovalent GaN/AlN system examined here the band-offset trends can be described quite accurately in terms of bulk properties, somewhat larger deviations should be expected for a system such as AlN/InN, which exhibits a very large lattice mismatch ($\sim 14\%$). In this case it would be ap-

TABLE II. Valence-band offsets (in eV) in pseudomorphic AlN/SiC and GaN/SiC zinc-blende (110) heterojunctions on an AlN substrate. The numbers in parentheses are results from calculations treating the Ga-3*d* orbitals as core states. Ideal configurations refer to heterojunctions generated using the SiC lattice parameter, and neglecting local atomic relaxation at the interface.

(110)	AlN/SiC	GaN/SiC
Pseudomorphic	1.71	0.55 (0.67)
Ideal	1.59	0.49 (0.59)

propriate also to consider higher-order deformation potentials to better describe the bulk contributions to the band offset.

B. Heterovalent systems

1. Nonpolar AlN/SiC and GaN/SiC (110) interfaces: deviations from the transitivity rule

Heterovalent quaternary heterojunctions, such as AlN/SiC and GaN/SiC, give rise to relatively complex interface configurations. One may envisage two types of abrupt interfaces: those including cation-anion bonds (Si-N, C-Al, or C-Ga) and those with cation-cation and/or anion-anion bonds (C-N, Si-Al, or Si-Ga). The former have been shown to be significantly more stable than the latter,^{18,19} consistent with the results of a transmission-electron microscopy (TEM) study of the 2H-AlN/6H-SiC(0001) interface.⁴⁴ In the present study we therefore focus on the AlN/SiC and GaN/SiC heterojunctions with Si-N and C-Al or C-Ga interfacial bonds.

The band offsets of the non-polar AlN/SiC and GaN/SiC(110) interfaces are presented in Table II. Results from calculations with and without local atomic relaxation are reported. Atomic relaxation increases the AlN/SiC and GaN/SiC (110) VBO's by about 0.1 eV. Using the experimental band-gap value of 2.4 eV for cubic SiC, the band alignments are of type I. Our results agree to within 0.1 eV with an existing linear-muffin-tin-orbital calculation for the ideal GaN/SiC(110) junction,¹⁸ and within 0.1–0.2 eV with a pseudopotential calculations for the pseudomorphic GaN/SiC(110) and AlN/SiC(110) junctions on a SiC substrate.²⁰

In Table II we also reported our VBO values for the GaN/SiC(110) interfaces with and without local atomic relaxation at the interface, and with the Ga-3*d* electrons treated as core states. The Ga-3*d* states are found to increase the VBO by ~ 0.1 eV. The Ga-3*d* correction is thus no more a purely bulk effect in the heterovalent GaN/SiC system: an interface-specific correction of about -0.1 eV partially cancels out the bulk GaN-3*d* shift discussed in Sec. III A 1. Our results with the Ga-3*d* electrons treated as core states (Tables I and II) indicate that, even without considering the effect of atomic relaxation, the transitivity rule is violated by 0.13 eV at the GaN/SiC, AlN/SiC, and AlN/GaN (110) interfaces.

The origin of this deviation can be easily identified by computing the potential lineups $\Delta V'(GaN/AlN)$, $\Delta V'(GaN/SiC)$, and $\Delta V'(AlN/SiC)$ resulting from a linear

superposition of the charge densities induced by single (110) atomic plane substitutions transforming the GaN/GaN(110) homojunction into GaN/AlN(110), GaN/SiC (110), and AlN/SiC (110) heterojunctions, respectively. In the absence of interaction between the planar substitutions, the transitivity rule would be verified. From the linear superposition of the charge densities we obtain, $\Delta V'(\text{AlN/GaN})=0.47$ eV, $\Delta V'(\text{SiC/GaN})=1.34$ eV, and $\Delta V'(\text{SiC/AlN})=0.87$ eV, which should be compared to the self-consistent values $\Delta V(\text{AlN/GaN})=0.49$ eV, $\Delta V(\text{SiC/GaN})=1.59$ eV, and $\Delta V(\text{SiC/AlN})=0.97$ eV. The comparison shows that, while intersite interactions have a negligible influence on the lineup of the common-anion GaN/AlN system, they affect the lineups of the heterovalent SiC/GaN and SiC/AlN systems by several tenths of an eV. These nonlinear contributions to the lineup at the heterovalent interfaces are responsible for the deviation from the transitivity rule, in agreement with our contentions in Sec. III A 1.

When local atomic relaxation at the interface is included, the deviation from the transitivity rule increases from 0.13 to 0.25 eV (without Ga-3d effects). The roughening at the (110) interface thus also has a non-negligible impact on the transitivity properties of these systems. When the Ga-3d electrons are treated as valence electrons, the total deviation is ~ 0.2 eV (0.02 eV) for the strained (ideal) junctions. Although for the specific systems considered here, the Ga-3d corrections tend to improve the transitivity properties of the ideal heterojunctions, this derives from a fortuitous cancellation between interface-specific contributions at two different interfaces: AlN/SiC and GaN/SiC. In general, therefore, the local chemistry at nitride interfaces with no common ion can induce nonbulk contributions to the VBO, and hence deviations from the transitivity rule, as large as several tenths of an eV, and this even at non-polar interfaces.

The changes of the AlN/SiC, GaN/SiC, and GaN/AlN (110) VBO's with strain and local interfacial atomic relaxation (Tables I and II) can be understood using a LRT description. In the case of AlN/SiC, only local atomic interfacial relaxation needs to be considered. For GaN/SiC and GaN/AlN, instead, both macroscopic strain and local interfacial relaxation have to be taken into account. The contribution of the macroscopic uniaxial strain in the GaN overlayer (4%) can be derived using the GaN deformations potentials determined in Sec. III A 2; the resulting VBO variations, including the band-edge splitting and the change in VBO_{ave} , are +0.20 and -0.20 eV, at the GaN/SiC(110) and GaN/AlN(110) interfaces, respectively. These corrections are bulk terms, which have thus no influence on the transitivity rule.

Within the LRT scheme, the displacement u_{\perp} of each atomic layer at the interface produces a shift

$$\Delta V_{relax} = 4\pi Z^* e^2 u_{\perp} / S \epsilon_{\infty} \quad (5)$$

in the potential lineup, where Z^* is the effective charge of the ions, S the surface per ion in the plane, and ϵ_{∞} the geometric average of the dielectric constants of the two crystals forming the junction.⁴⁵ In the GaN/AlN(110) junction, the N sublayer in the two planes closest to the interface are found to relax towards AlN. The resulting anion-cation relative dis-

placement is $\Delta u_{\perp} \approx 0.04$ a.u. In the AlN/SiC and GaN/SiC(110) junctions, the anion sublayers in the two planes closest to the interface relax toward SiC and the cation sublayers in the opposite direction. The resulting average anion-cation interlayer separation is about $\Delta u_{\perp} = -0.025$ (-0.055) a.u. at the AlN/SiC (GaN/SiC) interface. Using the theoretical values $\epsilon_{\infty}^{GaN} = 5.74$, $\epsilon_{\infty}^{AlN} = 4.61$, $\epsilon_{\infty}^{SiC} = 6.95$,⁴⁶ and $Z_{cation}^* = -Z_{anion}^* \approx 2.7$ in these materials,^{47,48} from Eq. (5) we obtain local atomic relaxation contributions to the VBO's of -0.31, +0.18, and +0.34 eV for the GaN/AlN, AlN/SiC, and GaN/SiC interfaces, respectively. The resulting total (strain plus local relaxation) change in the GaN/AlN, AlN/SiC, and GaN/SiC (110) VBO's are thus -0.11, +0.18, and +0.14 eV, respectively, in fair agreement with the first-principles results of -0.14, +0.12, and +0.06 eV (Tables I and II).

The large local atomic relaxation found at the GaN/AlN and GaN/SiC interfaces results from the large difference between the Ga and Al (or Si) covalent radii, or equivalently between the GaN and AlN (or SiC) lattice parameters. In fact, when the Ga-3d orbitals are treated as core states and the GaN lattice parameter becomes similar to those of AlN and SiC, the relative anion-cation displacements Δu_{\perp} in the two interfacial planes decrease significantly in magnitude (by ~ 0.03 a.u.). We note that, although the VBO contributions due to the macroscopic strain and local interfacial relaxation are both quite large, with the Ga-3d electrons treated as valence electrons, these terms are opposite in sign and partially cancel out. Because of this cancellation, the resulting total change in the VBO from the ideal to the relaxed situation is similar to that obtained neglecting the effects of the Ga-3d electrons.

Our study shows thus that non-negligible deviations from transitivity should be expected in general at nonpolar heterovalent nitride interfaces. Such deviations derive from local atomic relaxation as well as nonlinear effects associated with the local chemistry of the interfaces. Both contributions are found to be of the order of several tenths of an eV in the case of the GaN/SiC and AlN/SiC (110) systems.

2. Polar AlN/SiC and GaN/SiC (111) interfaces: atomic intermixing and local relaxation

(111)-oriented AlN/SiC and GaN/SiC heterojunctions may be envisaged either with a long (single) or short (triple) bond geometry at the interface. Since AlN/SiC and GaN/SiC heterojunctions are characterized by positive formation energies,^{19,20} here we will focus only on junctions with the long-bond geometry, which gives rise to the lowest density of bonds across the interface [see Fig. 5(a)]. As in Sec. III B 1 we consider only heterojunctions including Si-N or C-Al(Ga) interfacial bonds.

The abrupt polar AlN/SiC (111) and GaN/SiC (111) junctions are charged and therefore thermodynamically unstable. Charge neutrality can be restored by atomic intermixing at the interface.⁴⁹ The simplest atomic arrangements which give rise to neutral interfaces are those with one mixed N/C plane or one mixed Ga(Al)/Si plane. The corresponding neutral configurations, illustrated in Figs. 5(b) and 5(c) for the AlN/

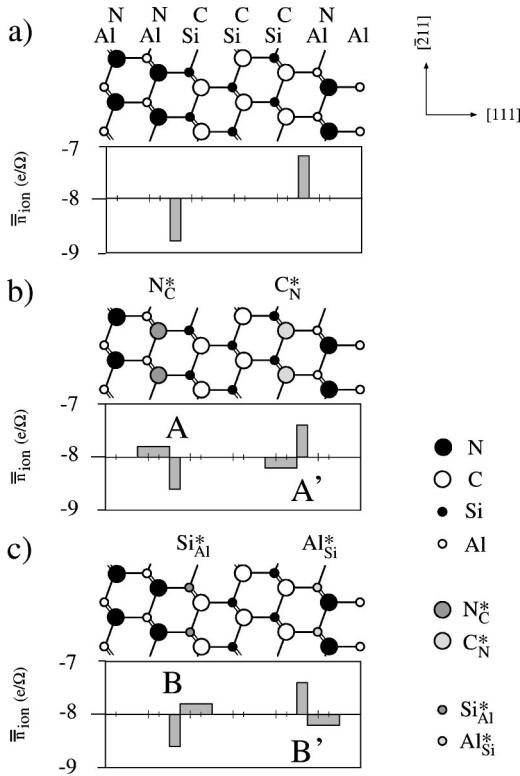


FIG. 5. Ball and stick representation of the zinc-blende AlN/SiC (111) heterostructures with charged, abrupt interfaces (a), neutral interfaces with one mixed C/N plane (b), and one mixed Al/Si plane (c). The symbol A_B^* indicates a mixed plane containing 75% A atoms and 25% B atoms. The macroscopic average of the ion-point-charge distribution in the junctions is shown in the lower part of the figures.

SiC system, are obtained by replacing 25% of N by C in the N plane at the abrupt N-Si interface or 25% of C by N in the C plane at the abrupt Al(Ga)-C interface (configurations A and A' , respectively), or similarly by replacing 25% of Si by Al(Ga) in the Si plane at the abrupt Si-N interface or 25% of Al(Ga) by Si in the Al(Ga) plane at the abrupt Al(Ga)-C interface (configurations B and B' , respectively). This type of intermixing neutralizes the junction leaving dipoles [which are opposite for the N/C and Al(Ga)/Si mixed layers] in the macroscopic average of the ion-point-charge distribution of the junctions (Fig. 5). We note that all possible neutral configurations that can be generated with two mixed N/C and Al/Si layers have a macroscopic charge profile that is a weighted average of those of A and B or A' and B' .²¹

We have computed the VBO of the neutral interfaces, shown in Fig. 5, with the mixed layers treated using the virtual crystal approximation, and with the Ga-3d orbitals treated as core states. The resulting band offsets are presented in Table III, with and without local atomic relaxation at the interface. In contrast to the case of the conventional semiconductor heterojunctions, local atomic relaxation has a drastic effect on the band offsets of these polar ionic interfaces. In the A and A' junctions, in particular, the local relaxation changes the offsets by as much as 0.6–0.7 eV. Although relaxation effects are somewhat smaller at the B and

TABLE III. Valence-band offset (in eV) at the AlN/SiC and GaN/SiC zinc-blende (111) interfaces. For the heterovalent (111) junctions, results are given for neutral interfaces with one mixed N/C plane (A, A') or one mixed Ga(Al)/Si plane (B, B') (see Fig. 5). Ideal configurations refer to heterojunctions without local atomic relaxation at the interface.

(111)	A	A'	B	B'
Pseudomorphic				
AlN/SiC	1.3	1.3	2.3	2.5
GaN/SiC ^a	0.4	0.3	1.3	1.4
Ideal				
AlN/SiC	0.6	0.7	2.4	2.7
GaN/SiC ^a	-0.3	-0.3	1.4	1.5

^aGa-3d orbitals treated as core states

B' interfaces, they change the band alignment from type II to type I at the AlN/SiC (111) interface. After relaxation, the band alignment is of type I at all interfaces.

For the ideal junctions, the LRT scheme²² predicts that the VBO's of the (111) interfaces with a dipole should differ from that of the nonpolar (110) interface by

$$\Delta V_{dip} = \pm \frac{\pi e^2}{2a\epsilon_\infty}, \quad (6)$$

where the plus (minus) sign corresponds to the dipole of the A and A' (B and B') interfaces. The corrections derived from Eq. (6) are ± 0.9 and ± 0.8 eV at the AlN/SiC and GaN/SiC interfaces, respectively. Using the averages of the *ab initio* values for the ideal A and A' interfaces and for the B and B' interfaces, we obtain -0.9 and $+1.0$ eV for AlN/SiC and -0.9 and $+0.9$ eV for GaN/SiC, not too far from the linear-response estimates. However, we note that deviations from the average values can be as large as 0.2 eV. Such deviations are of the same order of magnitude as the deviations from the transitivity rule due to the details of the local interface chemistry that we discussed in the previous section. Following the LRT scheme, all neutral configurations with two mixed N/C and Al(Ga)/Si layers should have a VBO which is intermediate between those of A and B or A' and B' . We expect such predictions to hold to within ~ 0.2 eV.

The changes in the interplanar spacings at the AlN/SiC A and B interfaces are illustrated in Fig. 6 (similar relaxation patterns are found at the A' and B' interfaces). Analogous trends are also observed in the GaN/SiC junctions. In the AlN/SiC A and A' junctions, the mixed anion plane is found to relax toward the SiC by about 0.07 a.u., and the cation plane closest to the interface relaxes, by about the same amount, in the opposite direction. Both displacements tend to increase the AlN/SiC VBO. The total change in the VBO evaluated from LRT is $\Delta V_{relax} = 0.8$ eV, in good agreement with the *ab initio* results. The displacements of the planes closest to the interface are about two times smaller for the B and B' interfaces, and the cation and anion planes both relax towards SiC. The corresponding relaxation contributions to the VBO tend thus to cancel each other, and the relaxation has therefore a much smaller impact on the VBO in these

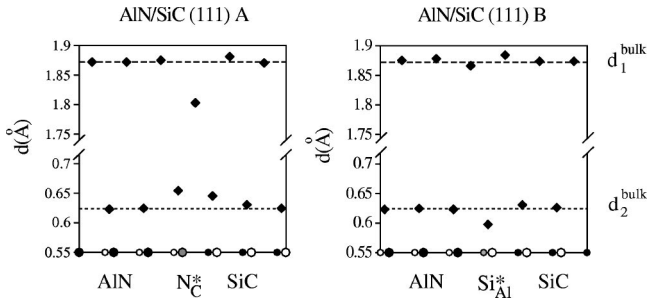


FIG. 6. Equilibrium interplanar spacings in the AlN/SiC(111) heterojunctions with neutral interfaces containing one mixed N/C layer (A) and one mixed Al/Si layer (B). The sequence of atomic layer is indicated at the bottom of each graph. The dashed (dotted) lines indicates the bulk interplanar spacing associated with the long (short) bond projection along the [111] axis.

junctions. We attribute the relaxation at the polar AlN/SiC and GaN/SiC (111) interfaces mainly to electrostatic forces, as the relaxation predominantly decreases the electrostatic component of the total energy. The larger relaxation observed at interfaces *A* and *A'* as compared to interfaces *B* and *B'* is ascribed to the larger electrostatic potential discontinuity ΔV (~ 2 eV versus less than 1 eV), and hence the larger electric field found at the *A* and *A'* junctions.

In summary, giant local ionic relaxation effects, approaching 1 eV, are found at polar heterovalent nitride interfaces, which tend to reduce the local electric field present at the junction. This behavior derives from the high ionicity of the nitride interfaces, and is rather different from that observed in the conventional semiconductor heterojunctions, where atomic interfacial relaxation typically modifies the offsets by 0.1–0.2 eV. We note that Stadele *et al.* also reported considerable VBO changes (up to 0.9 eV) induced by local atomic relaxation at the polar (100)-oriented GaN/SiC and AlN/SiC interfaces.¹⁹ In principle, interfacial relaxation depends on the local chemistry established at the polar interface, which in turn depends on the interface crystallographic orientation. The results of Stadele *et al.*, however, showed relaxation trends which were qualitatively similar to what we find for the (111)-oriented junctions. They obtained a large/small increase in the VBO at the anion/cation intermixed interfaces, which correspond to the largest/smallest potential lineup, in agreement with our interpretation of this effect.

IV. WURTZITE VS ZINC-BLENDE HETEROSTRUCTURES

The zinc-blende and hexagonal polytypes, which include the 2H (wurtzite) and 6H structures, consist of identical atomic layers with different stacking sequences along the hexagonal (111) or (0001) axes. These different stacking sequences give rise to very different band gaps. In the wurtzite phase, the bandgaps of GaN, AlN, and SiC are 3.6, 6.3, and 3.3 eV, respectively,^{33,31} i.e., 0.4, 1.4, and 0.9 eV larger than in the cubic phase. We have investigated the influence on the VBO of such large band gap changes induced by a transformation from zinc-blende (111) to wurtzite (0001) crystal structures in AlN/GaN, AlN/SiC, and GaN/SiC heterojunctions. We considered pseudomorphic heterojunctions grown

TABLE IV. Valence-band offset (in eV) in pseudomorphic wurtzite GaN/AlN, AlN/SiC, and GaN/SiC, (0001) heterojunctions with SiC or AlN substrates. For the heterovalent AlN/SiC and GaN/SiC heterojunctions, neutral interfaces with one mixed N/C layer (*A, A'*) and one mixed Al/Si layer (*B, B'*) have been considered.

GaN/AlN	AlN/SiC		GaN/SiC ^a	
	<i>A, A'</i>	<i>B, B'</i>	<i>A, A'</i>	<i>B, B'</i>
1.1	1.3, 1.4	2.2, 2.5	0.4, 0.3	1.3, 1.4

^aGa-3*d* orbitals treated as core states.

on a SiC substrate. For the heterovalent AlN/SiC and GaN/SiC systems, we examined the same types of atomic intermixing as for the zinc-blende (111) heterojunctions (corresponding to the *A, A'*, *B*, and *B'* interfaces). The calculated wurtzite VBO's, including local atomic relaxation at the interface, are displayed in Table IV.

Notwithstanding the large band-gap differences between the cubic and hexagonal structures—which change the band-gap discontinuity by 1.0, 0.5, and 0.3 eV in AlN/GaN, AlN/SiC, and GaN/SiC heterojunctions, respectively—the VBO's of the (0001) and (111) systems are identical, except for the AlN/SiC *A'* and *B* interfaces, where the VBO's differ by only 0.1 eV. The large band-gap modifications induced by the change from cubic to hexagonal polytypes are thus predominantly absorbed by the conduction band offset.

In order to understand and generalize this trend, we first investigated the variation produced by 3H/2H stacking faults on the potential lineup in the transformation 3C-AlN/3C-SiC \rightarrow 2H-AlN/3C-SiC \rightarrow 2H-AlN/2H-SiC. The potential lineups of the 2H/3C, 2H/2H, and 3C/3C heterojunctions were found to be identical to within ~ 50 meV. We also examined 2H/3C homojunctions in SiC and AlN, and obtained potential discontinuities that did not exceed 0.04 eV. This is in general agreement with the results of other *ab initio* studies of the lineups across 3C/2H homojunctions in ionic materials.^{50–52} One may safely conclude thus that in ionic systems, in general, stacking faults have a very small impact on ΔV , both in homo-junctions and in heterojunctions.

We then examined the impact of the 3C \rightarrow 2H structural transformation on the band-structure terms in AlN, SiC, and GaN crystals. In Fig. 7 we show the alignment of the zincblende and wurtzite LDA densities of states at 2H/3C AlN, SiC, and GaN homojunctions, as obtained with a potential lineup $\Delta V \sim 0$. For all systems, the matching of the 2H and 3C density of states features and band-edge positions in the valence band is quite striking, and in contrast with the situation of the conduction band. This is because the environment of each atom in the cubic and hexagonal structures differs only beyond the first neighbors, and, unlike the bonding orbitals, which are highly localized on the anions, the more delocalized conduction states are quite sensitive to the bonding geometry of the neighboring atoms. The results in Fig. 7 for the band-structure terms, together with the very small impact of stacking faults on ΔV , indicate that for such ionic systems in general the change in the band-gap discontinuity associated with a cubic to hexagonal structural modi-

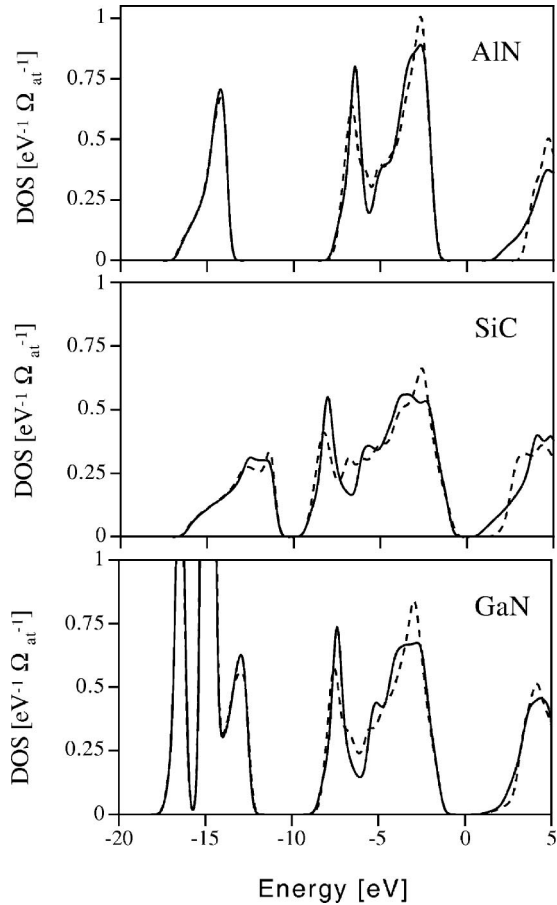


FIG. 7. Density of states of the 3C (solid line) and 2H (dashed line) crystals in the 3C-AlN/2H-AlN and 3C-SiC/2H-SiC junctions with the band alignment obtained from the self-consistent calculation for the interfaces. The zero of energy has been chosen at the midgap value of the 3C structure.

fication will be selectively found in the conduction-band offset, leaving the VBO essentially unchanged.

We may use this property to compare our computed VBO values to previous theoretical data for wurtzite GaN/AlN(0001) heterojunctions coherently strained to different substrate lattice constants. Based on our calculated values for the GaN/AlN(111) VBO and for the GaN and AlN deformation potentials, and considering a +4% (−4%) uniaxial deformation, $\epsilon_{\perp} - \epsilon_{\parallel}$, for GaN on AlN (AlN on GaN) in pseudomorphic (111) heterostructures, we predict VBO values of 1.1, 0.9, and 0.7 eV for GaN/AlN (0001) and (111) heterojunctions with $a_{\parallel} = a_{\text{AlN}}$, $\frac{1}{2}(a_{\text{AlN}} + a_{\text{GaN}})$, and a_{GaN} , respectively. Taking into account a ± 0.2 -eV uncertainty on our VBO's, these predictions are consistent with the value of 0.81-eV calculated by Wei and Zunger, using as in-plane lattice parameter the average between the AlN and GaN lattice constants.¹² Our values are instead very different from those reported by Bernardini and Fiorentini, who obtained VBO's of 0.20 (0.85) eV for GaN/AlN(0001) heterojunctions coherently strained to GaN (AlN).¹⁶ This may be due in part to the use of different pseudopotentials. Bernardini and Fiorentini employed ultrasoft pseudopotentials, which lead to 1% larger GaN lattice parameters and a misfit $\Delta a/a$ of 4%,

instead of 3%, between AlN and GaN. Based on our results in Sec. III A 2, such a difference could account for changes of 0.1 to 0.2 eV in the VBO and in its variation with the substrate.

V. DISCUSSION

The experimental data indicate a type-I band alignment for the isovalent 2H-GaN/2H-AlN(0001) heterojunction,^{3–8} with VBO values ranging from 0.15 eV (Ref. 8) to 1.4 eV (Refs. 4 and 5). Although the type-I alignment agrees with our prediction, the large spreading of the experimental values is somewhat surprising. Our study indicates that, except for strain effects (which could account for a ~ 0.4 -eV variation at most in the GaN/AlN VBO), the offsets of these isovalent nitride heterojunctions should be relatively insensitive to interface-specific features.

It should be noted, however, that except for an experimental GaN/AlN VBO estimate of 0.5 eV³—derived from GaN:Fe and AlN:Fe photoluminescence spectra using the iron -0 acceptor level as a common reference level—and a rough estimate of 1.4 eV⁴—obtained from a fit to cathodoluminescence data for strained GaN/AlN heterostructures on SiC—all direct measurements of the GaN/AlN VBO were obtained by photoemission experiments.^{5–8} In the photoemission experiments, the VBO is obtained from two independent sets of data: (i) measurements of the energy difference between the valence-band edge and an intrinsic atomic core level in each bulk material, and (ii) measurements of the energy difference between the reference core levels of the two materials in the actual heterojunction. Inspection of the data indicates⁷ that most of the discrepancy in the photoemission measurements of the VBO actually derives from the bulk contributions (i), and not from interface-specific terms. As discussed in Refs. 7 and 8, such a discrepancy should be attributed primarily to differences in the material quality of the nitrides and their surfaces (such as defects, strain, and deviation from stoichiometry), and also, to some extent, to complications in the interpretation of the photoemission measurements due to polarization fields.

In view of the scattering in the experimental data, we may thus compare our theoretical result only to a range of experimental values. Our prediction for the VBO of the relaxed GaN/AlN system (0.87 eV) is, in fact, well within the range of the VBO values measured by photoemission (0.15–1.4 eV). Here we quoted the theoretical value obtained for the relaxed system, as in the photoemission measurements, the band-structure contributions (i) are measured in the relaxed bulk materials. Furthermore, based on recent experiments,⁵³ relaxed growth occurs in GaN/SiC heterojunctions for GaN epilayers as thin as 7 Å. This indicates that most overlayers used in photoemission experiments to determine the interface-related contribution (ii) are actually also closer to the fully relaxed case than to a pseudomorphic situation.

In their photoemission study, Martin *et al.*⁶ examined the transitivity properties of the band offsets in GaN/AlN, InN/GaN, and InN/AlN heterojunctions. They obtained VBO values of 0.7 ± 0.24 , 1.05 ± 0.25 , and 1.81 ± 0.20 eV for GaN/AlN, InN/GaN, and InN/AlN, respectively, that obey the

transitivity rule to within experimental uncertainty. Based on our results, a transitive behavior is indeed expected for isovalent nitride systems, provided the heterojunctions are either fully relaxed or coherently strained to a common in-plane lattice parameter. The systems examined in Ref. 6 correspond to different underlayers with different in-plane lattice parameters. The experimentally observed transitivity therefore also suggests the presence of relaxed overlayers, in agreement with our above contentions.

Concerning heterovalent systems, band-offset data are available for 2H-AlN/6H-SiC (0001) and 2H-GaN/6H-SiC (0001) heterojunctions, and for 2H-GaN(0001)/3C-SiC(111) and 2H-AlN(0001)/3C-SiC(111) heterojunctions.^{8–11} In view of the results of Sec. V, such data may be compared to our theoretical values for the VBO of the 3C/3C (111) or 2H/2H (0001) systems. For GaN and AlN overlayers grown on Si-terminated SiC substrates, photoemission measurements by Rizzi *et al.*⁸ provided VBO values of $(1.5–1.7) \pm 0.1$ eV and $(0.7–0.9) \pm 0.1$ eV in 2H-AlN/6H-SiC and 2H-GaN/6H-SiC systems, respectively. These photoemission results are consistent with those by King *et al.*⁹: $(1.2–1.5) \pm 0.2$ eV for 2H-AlN/6H-SiC and $(0.5–0.8) \pm 0.1$ eV for 2H-GaN/3C-SiC, using the same type of substrates, namely, Si-terminated on-axis SiC substrates. For 2H-GaN/6H-SiC, relatively similar values of 0.48 ± 0.1 (Ref. 10) and 0.67 eV (Ref. 11) were obtained also by transport measurements. Although all of the above data are consistent with the theoretical range of values we obtain for neutral⁵⁴ heterojunctions including 1–2 mixed layers [1.3–2.5 eV for AlN/SiC(0001) and 0.3–1.4 eV for GaN/SiC (0001)], the experimental values are clearly in the lowest portion of our energy window, which corresponds to interfaces involving anion (N/C) rather than cation [Si/Al(Ga)] intermixing. The growth of GaN and AlN on Si-terminated SiC substrates thus appears to favor anion intermixing, a conclusion that is not inconsistent with TEM and spectroscopic measurements on these systems,^{9,44,53} and with recent *ab initio* simulations of nitrogen deposition on Si-terminated SiC.⁵⁵

For the 2H-AlN/6H-SiC system, King *et al.*⁹ performed an extensive study of the effects of different growth sequences (SiC on AlN versus AlN on SiC), substrate cut (on-cut axis versus off-cut axis), and surface termination/reconstruction on the VBO. For SiC deposited on Al-terminated AlN(0001) surfaces, they measured VBO values of $(1.9–2.0) \pm 0.2$ eV. In these experiments, the AlN surfaces were pre-exposed to SiH₄ prior to growth of the SiC film, in order to favor cation intermixing. The resulting VBO values are in the upper part of our proposed range. This indicates predominant cation intermixing, consistent with the expected influence the surface/interface preparation method.⁹

The effect of AlN growth on off-cut Si-terminated SiC substrates was also examined, and found to decrease the AlN/GaN VBO by as much as ~ 0.5 eV.⁹ In principle, considering the effect produced, within the LRT scheme, by diatomic steps in the charge distribution at the interfaces, one would expect no change in the VBO. However, as emphasized in Ref. 9, growth on off-axis substrates generates a substantial amount of defects. We also saw that local atomic interfacial relaxation strongly depends on the local chemistry (type of

defects) present at the interface, and produces changes in the VBO at polar heterovalent interfaces comparable to those observed experimentally with off-cut substrates. Interfacial defects and the resulting local atomic interfacial relaxation may therefore very well be responsible for the VBO modifications observed with off-cut substrates.

Finally, for AlN films grown on on-axis C-terminated (000 $\bar{1}$) SiC wafers, King *et al.* obtained VBO values as low as $(0.6–0.7) \pm 0.2$ eV [$(1.0–1.1) \pm 0.2$ eV] for SiC surfaces exposed to NH₄ (Al) prior to AlN growth.⁹ These values are almost 2 eV smaller than the calculated VBO of neutral interfaces with one intermixed cation layer, and also somewhat smaller than those with one intermixed anion layer. It should be mentioned, however, that in the experiment, after the cleaning procedure and prior to AlN deposition, the SiC underlayers exhibited a Si-terminated (1 \times 1) surface,⁹ which is surprising for a C-terminated (000 $\bar{1}$) wafer. The expected long (single) and short (triple) bond sequence along (000 $\bar{1}$) of a C-terminated wafer is Si–C–Si–C–Si–C, with a short bond at the surface for stability reasons. Such a stacking naturally leads to a Si-terminated surface with a long bond at the surface (Si–C–Si–C–Si), which is highly unstable. It is very likely thus, that the observed “Si-terminated surface” of the C-terminated SiC (000 $\bar{1}$) wafer has a complex nonstoichiometric atomic structure, possibly involving more than one Si layer. The resulting AlN/SiC interface may therefore have a rather complex atomic geometry, involving more than two intermixed layers. Although high formation energies are expected for heterojunctions exhibiting large dipoles, generated by intermixing over more than two atomic layers, such configurations may actually form at some surfaces, for kinetic reasons.

VI. CONCLUSIONS

By means of first-principles calculations we have studied various properties of the band offsets in nitride heterojunctions, including their dependence on interface orientation, heterovalency, and polytype. We considered selected prototypic isovalent (GaN/AlN) and heterovalent (GaN/SiC and AlN/SiC) systems with zinc-blende, wurtzite, and mixed zinc-blende/wurtzite structures.

In the isovalent zincblende GaN/AlN (100), (110) and (111) heterojunctions, the band offsets are relatively insensitive (to within 0.1 eV) to the orientation and structural details of the interface, consistent with the trend established from linear-response theory for the conventional, smaller-gap, semiconductor heterojunctions. For the ionic nitride systems, however, the presence of common (N) ions is essential to insure a transitive behavior of the band offsets. Strain effects have an important impact on the band discontinuities, producing modifications as large as 0.4 eV in the offsets of coherently strained AlN/GaN(100) and GaN/AlN (100) heterojunctions. These effects, however, are determined by the bulk properties (deformation potentials) of the interface constituents, as opposed to interface-specific effects.

In the nonpolar heterovalent GaN/SiC(110) and AlN/SiC(110) systems, the offsets show significant deviations (a

few tenths on an eV) from the predictions of the transitivity rule. These deviations derive from both the local chemistry and the local atomic relaxation at the interfaces.

At the polar GaN/SiC(111) and AlN/SiC(111) junctions, the band alignment critically depends on the interface chemical composition, and differences in the offsets as large as 1 eV are found between neutral interfaces including mixed anion (N/C) and mixed cation [Al(Ga)/Si] planes. Local atomic relaxation also plays a major role in determining the band offsets at these interfaces. This is in contrast to the case of the conventional semiconductor heterojunctions, and follows from the high ionicity of the heterovalent nitride systems. However, even in these highly ionic systems, provided local atomic relaxation is taken into account, the band-offset dependence on interface orientation and heterovalency can still be qualitatively explained using a linear-response-theory approach.

Finally, a change from zincblende to wurtzite crystal structure in GaN/AlN, GaN/SiC, AlN/SiC (111) and (0001) heterojunctions selectively affects the conduction-band offset, and has only a minor influence on the valence discontinuity.

This behavior derives from two general properties observed in highly ionic systems, and that apply to other hexagonal polytypes. First, the stacking faults involved in the transformations from cubic to hexagonal polytypes have only a negligible influence on the potential lineup. Second, the bulk band-structure terms involved in the VBO remain essentially invariant in fourfold-coordinated cubic and hexagonal crystal structures. We may therefore conclude that, in general, the change in the band-gap discontinuity resulting from a cubic (111) to hexagonal (0001) structural modification in a wide-gap-semiconductor heterojunction will be selectively found in the conduction-band offset.

ACKNOWLEDGMENTS

We would like to acknowledge support for this work by the Swiss National Science Foundation under Grant No. 20-55811.98. We thank A. Franciosi, J. Bardi, and X. Blase for useful discussions. Computations were performed on the NEC-SX4 at the CSCS in Manno.

*Present address: Biochemisches Institut der Universität Zürich, Winterthurerstrasse 190, CH-8057 Zürich, Switzerland.

¹S. Nakamura, MRS Bull. **XXIII**, No. 5, 37 (1998); also see review articles in MRS Bull. **XXII**, No. 2 (1997).

²F.A. Ponce, B. Krusor, J.S. Major, W.E. Plano, and D.F. Welch, Appl. Phys. Lett. **67**, 410 (1995).

³J. Baur, K. Maier, M. Kunzer, U. Kaufmann, and J. Schneider, Appl. Phys. Lett. **65**, 2211 (1994).

⁴Z. Sitar, M.J. Paisley, B. Yan, F. Davis, J. Ruan, and J.W. Choyke, Thin Solid Films **200**, 311 (1991).

⁵J.R. Waldrop and R.W. Grant, Appl. Phys. Lett. **68**, 2879 (1996); R. A. Beach, E. C. Piquette, R. W. Grant, and T. C. McGill, in *Nitride Semiconductors*, edited by F. A. Ponce, S. P. Ven Buars, B.K. Meyer, S. Nakamura, and S. Strile, MRS Symposia Proceedings No. 482 (Materials Research Society, Pittsburgh, 1998), p. 775.

⁶G. Martin, A. Botchkarev, A. Rockett, H. Morkoc, and A. Botchkarev, Appl. Phys. Lett. **68**, 2541 (1996).

⁷S.W. King, C. Ronning, R.F. Davis, M.C. Benjamin, and R.J. Nemanich, J. Appl. Phys. **84**, 2086 (1998).

⁸A. Rizzi, R. Lantier, F. Monti, H. Lüth, F. Della Sala, A. Di Carlo, and P. Lugli, J. Vac. Sci. Technol. B **17**, 1674 (1999); R. Lantier, F. Boscherini, A. Rizzi, F. D'Acapito, S. Mobilio, and H. Lüth, Phys. Status Solidi A **176**, 615 (1999).

⁹S.W. King, R.F. Davis, C. Ronning, M.C. Benjamin, and R.J. Nemanich, J. Appl. Phys. **86**, 4483 (1999); S.W. King, R.F. Davis, C. Ronning, and R.J. Nemanich, J. Electron. Mater. **28**, L34 (1999).

¹⁰J.T. Torvik, M. Leksono, J.I. Pankove, B. Van Zeghbroeck, H.M. Ng, and T.D. Moustakas, Appl. Phys. Lett. **72**, 1371 (1998).

¹¹M. Topf, D. Meister, I. Dirnstorfer, G. Steude, S. Fischer, B.K. Meyer, A. Krtschil, H. Witte, J. Christen, T.U. Kampen, and W. Mönch, Mater. Sci. Eng., B **50**, 302 (1997).

¹²S.-H. Wei and A. Zunger, Appl. Phys. Lett. **69**, 2719 (1996).

¹³C.G. van de Walle and J. Neugebauer, Appl. Phys. Lett. **70**, 2577 (1997).

¹⁴M.B. Nardelli, K. Rapcewicz, and J. Bernholc, Phys. Rev. B **55**, R7323 (1997).

¹⁵E.A. Albanesi, W.R. Lambrecht, and B. Segall, J. Vac. Sci. Technol. B **12**, 2470 (1994).

¹⁶F. Bernardini and V. Fiorentini, Phys. Rev. B **57**, R9427 (1998); A. Satta, V. Fiorentini, A. Bosin, F. Meloni, and D. Vanderbilt, in *Gallium Nitride and Related Materials*, edited by R. D. Dupuis, J. A. Edmond, F. A. Ponce, and S. Nakamura, MR Symposia Proceeding No. 395 (Materials Research Society, Pittsburgh 1996), P. 515.

¹⁷J. A. Majewski and M. Städele, in *Nitride Semiconductors* (Ref. 5), p. 917.

¹⁸W.R.L. Lambrecht and B. Segall, Phys. Rev. B **43**, 7070 (1991); E. A. Albanesi, W. R. Lambrecht, and B. Segall, in *Diamond, SiC and Nitride Wide Bandgap Semiconductors*, edited by C. H. Carter, G. Gildenblat, S. Nakamura, and R. J. Nemanich, MRS Symposia Proceedings No. 339 (Materials Research Society, Pittsburgh, 1994), P. 607.

¹⁹M. Städele, J.A. Majewski, and P. Vogl, Phys. Rev. B **56**, 6911 (1997).

²⁰J. A. Majewski, M. Städele, and P. Vogl, in *Proceedings of the XXIII International Conference on the Physics of Semiconductors*, edited by M. Scheffler and R. Zimmermann (World Scientific, Singapore, 1996), p. 983.

²¹Ph. Ferrara, N. Binggeli, and A. Baldereschi, Phys. Rev. B **55**, R7418 (1997).

²²S. Baroni, R. Resta, A. Baldereschi and M. Peressi, in *Spectroscopy of Semiconductor Microstructures*, edited by G. Fasol, A. Fasolino and P. Lugli (Plenum, New York, 1989); M. Peressi, S. Baroni, A. Baldereschi, and R. Resta, Phys. Rev. B **41**, 12106 (1990).

²³D.M. Ceperley and B.J. Alder, Phys. Rev. Lett. **45**, 566 (1980); J. Perdew and A. Zunger, Phys. Rev. B **23**, 5048 (1981).

²⁴N. Troullier and J.L. Martins, Phys. Rev. B **43**, 1993 (1991).

²⁵L. Kleinman and P.M. Bylander, Phys. Rev. Lett. **48**, 1425 (1982).

- ²⁶H.J. Monkhorst and J.D. Pack, Phys. Rev. B **13**, 5188 (1976); S. Froyen, *ibid.* **39**, 3168 (1989).
- ²⁷G. L. Harris, in *Properties of Silicon Carbide*, edited by G. L. Harris (INSPEC, London, 1995), p. 4.
- ²⁸W. J. Meng, in *Properties of Group III Nitrides*, edited by J. H. Edgar (INSPEC, London, 1994), p. 22; I. Akasaki and H. Amano, in *ibid.*, p. 30.
- ²⁹K. Kim, W.R.L. Lambrecht, and B. Segall, Phys. Rev. B **53**, 16310 (1996); **56**, 7018 (1997).
- ³⁰M. Peressi, N. Binggeli, and A. Baldereschi, J. Phys. D **31**, 1273 (1998).
- ³¹S. Yoshida, in *Properties of Silicon Carbide* (Ref. 27) p. 74.
- ³²A self-energy correction of -0.2 eV on the valence-band edge of cubic GaN was calculated by M. Palummo *et al.*, Europhys. Lett. **26**, 607 (1994). Assuming a linear scaling with the band gap, one obtains rough estimates for the many-body corrections on the AlN/GaN, AlN/SiC, and GaN/SiC VBO's of $0.1-0.2$ eV.
- ³³W. R. L. Lambrecht and B. Segall, in *Properties of Group III Nitrides* (Ref. 28), pp. 135 and 141; the authors gave an estimate for the AlN-3C band gap using the measured AlN-2H value and a theoretical prediction for the 3C and 2H band-gap difference.
- ³⁴Preliminary results were presented in N. Binggeli, Ph. Ferrara, and A. Baldereschi, in *Nitride Semiconductors* (Ref. 5), p. 911; we note that in Table I of that reference, the values for the AlN/GaN (100) and (110) orientations interchanged by mistake.
- ³⁵S.-H. Wei and A. Zunger, Phys. Rev. Lett. **59**, 144 (1987).
- ³⁶S.G. Louie, S. Froyen, and M.L. Cohen, Phys. Rev. B **26**, 1738 (1982).
- ³⁷A. Baldereschi, M. Peressi, S. Baroni, and R. Resta, in *Proceedings of the International School of Physics "Enrico Fermi" (Course CXVII, Varenna, 1991): Semiconductor Superlattices and Interfaces*, edited by L. Miglio and A. Stella (Academic, New York, 1993), p. 59.
- ³⁸C. van de Walle, Phys. Rev. B **39**, 1871 (1989).
- ³⁹C. van de Walle and R. Martin, Phys. Rev. Lett. **62**, 2028 (1989).
- ⁴⁰R. Resta, L. Colombo, and S. Baroni, Phys. Rev. B **41**, 12358 (1990).
- ⁴¹For the internal strain parameter ξ , we used the theoretical values $\xi^{\text{GaN}}=0.5$ and $\xi^{\text{AlN}}=0.4$.
- ⁴²J. Bardi, N. Binggeli, and A. Baldereschi, Phys. Rev. B **54**, R11102 (1996).
- ⁴³From the GaN and AlN volume changes ($+10\%$), and using our computed values of the deformation potentials, we predict a VBO variation of -0.15 eV, which accounts quite well for this effect.
- ⁴⁴F.A. Ponce, C.G. Van de Walle, and J.E. Northrup, Phys. Rev. B **53**, 7473 (1996).
- ⁴⁵M. Peressi, L. Colombo, R. Resta, S. Baroni, and A. Baldereschi, Phys. Rev. B **48**, 12 047 (1993).
- ⁴⁶J. Chen, Z.H. Levine, and J.W. Wilkins, Phys. Rev. B **50**, 11514 (1994); Appl. Phys. Lett. **66**, 1129 (1995).
- ⁴⁷T. Sengstag, N. Binggeli and A. Baldereschi, Phys. Rev. B **52**, R8613 (1995).
- ⁴⁸F. Bernardini, V. Fiorentini, and D. Vanderbilt, Phys. Rev. B **56**, R10024 (1997).
- ⁴⁹W.A. Harrison, E.A. Kraut, J.R. Waldrop, and R.W. Grant, Phys. Rev. B **18**, 4402 (1978); K. Kunc and R.M. Martin, *ibid.* **24**, 3445 (1981).
- ⁵⁰A. Qteish, V. Heine, and R.J. Needs, Phys. Rev. B **45**, 6534 (1992).
- ⁵¹S. Ke, J. Zi, K. Zhang, and X. Xie, Phys. Rev. B **54**, 8789 (1996).
- ⁵²M. Posternak, A. Baldereschi, A. Catellani, and R. Resta, Phys. Rev. Lett. **64**, 1777 (1990).
- ⁵³F. Boscherini, R. Lantier, A. Rizzi, F. D'Acapito, and S. Mobilio, Appl. Phys. Lett. **74**, 3308 (1999).
- ⁵⁴The surface charge induced by the ionic distribution of the abrupt polar heterovalent interfaces and the surface polarization charge induced by the ferroelectric nature of the heterojunction materials should not be confused. The former is $1-2$ orders of magnitude larger than the latter.
- ⁵⁵G. Galli, A. Catellani, and F. Gygi, Phys. Rev. Lett. **83**, 2006 (1999).